

CHARMED MESON PHYSICS ACCESSIBLE TO AN $L=10^{33} \text{ cm}^{-2} \text{ sec}^{-1}$
 e^+e^- COLLIDER OPERATING NEAR CHARM THRESHOLD*

RAFE H. SCHINDLER

Stanford Linear Accelerator Center

Stanford University, Stanford, CA 94309 USA

ABSTRACT

In this report, the potential for dedicated charmed D^0 , D^+ and D_s meson physics in a high-luminosity e^+e^- collider operated near charm threshold is explored. The construction of such a high-luminosity collider or **Tau-Charm Factory** in conjunction with a new detector whose design draws heavily on the extensive operational experience of previous detectors at SPEAR, could achieve three orders-of-magnitude improvement in sensitivity in most areas of charmed meson studies.

*Invited talk presented at Les Rencontres de Physique de la
Vallee D'Aoste: Results and Perspectives in Particle Physics,
LaThuile, Italy, February 26-March 4, 1989.*

*Work supported by the Department of Energy, contract DE-AC03-76SF00515.

The Tau-Charm Factory is described in detail in these proceedings by M. Perl.¹⁾ Briefly, we assume an e^+e^- collider operating between $\sqrt{s} = 3.0$ and 4.4 GeV/c² with a luminosity $L = 10^{33}$ sec⁻¹ that peaks at about 4.0 GeV/c². We assume that with a dedicated injector, the injection time can be optimized against beam lifetimes to allow us to run the machine with $L_{peak} \approx L_{avg}$.²⁾ We therefore choose 5000 hours of fully efficient data-taking as our definition of one running year at each energy.³⁾

Three distinct center-of-mass energies (3.770, 4.028, and 4.140 GeV/c²) are chosen for the study of charmed meson production. The production cross sections and rates are summarized in Table I.

Table I. Charm production cross sections and event rates.

Center-of-Mass Energy (GeV/c)	Produced Species	Cross Section (nb)	Pairs Produced ($\times 10^{-7}$)
3.770	$D^0\bar{D}^0$	5.8 ± 0.8	5.0
3.770	D^+D^-	4.2 ± 0.7	4.0
4.028	$D_s\bar{D}_s$	0.7 ± 0.2	1.2
4.140	$D_s\bar{D}_s^*$	0.9 ± 0.2	1.6

In addition, the option to run just below $D^0\bar{D}^0$ threshold at 3.728 GeV/c² exists, to provide information on backgrounds that would otherwise introduce systematic uncertainties by requiring detailed reliance on fragmentation Monte Carlos.

There are three primary reasons for studying charm at or near threshold, as opposed to studies in the continuum. First, as seen in Table I, production cross sections of charm are large and well measured.⁴⁾ Charm production at higher energies in e^+e^- is smaller (see Table II) and production is not exclusive.

Second, the production processes near threshold are all *exclusive* in nature. Just above threshold, all production is pairlike with no extra particles in the fragmentation chain. This implies low combinatoric backgrounds and, more importantly, the unique pair-production

Table II. Charm in the continuum and at the $\Upsilon(4S)$ for $\int Ldt = 10^{40} \text{ cm}^{-2}$.

Species	Continuum Cross Section (nb)	Produced $\sigma_c = 2.66 \text{ nb}$ ($\times 10^{-7}$)	Produced $\sigma_b = 2.30 \text{ nb}$ ($\times 10^{-7}$)	Tau-Charm Year ($\times 10^{-7}$)
$D^0 + \bar{D}^0$	1.3	1.1	1.0	10.
D^\pm	0.6	0.5	0.4	8.0
D_s^\pm	0.4	0.3	0.3	3.2

kinematics. These kinematics may be exploited to separate noncharm from charm events as well as providing the essential background rejection (in addition to that attainable without the need to construct highly specialized detectors) for the proposed study of rare processes. Finally, only at low energy is full knowledge of all physics backgrounds both possible and *independently* verifiable by small changes in center-of-mass energies.

The primary techniques employed in most studies of charm near threshold are either the *single* or *double tagging* method. In the single tag technique, one charmed meson is *tagged* by reconstructing its mass. Once one meson is tagged, the recoil system is *a priori* known to be another charmed meson with a known charm (*e.g.*, flavor tagged), and by kinematics, a known 4-momentum. Backgrounds that might exist in studying properties of the recoiling system are suppressed in two ways. First, the event has been charm *enriched* by selection of the tag, hence noncharm backgrounds are severely reduced. It is reasonable to assume that one can achieve a contamination in the tag sample of $\leq 10\%$.⁵⁾ Second, by reconstructing one-half the event as a tag, the combinatorics in the recoil half are significantly reduced. Unlike vertex-finding (proposed to reduce combinatorics at higher energies), there is no confusion here from tracks in the first half of the event. This reduction means that it is reasonable to assume that in most analyses, one can achieve combinatoric backgrounds very close to zero,⁶⁾ after suffering only a small and known loss of signal efficiency due to the tagging requirement.

Double tagging means that all or part of both mesons are reconstructed in an event. The strength of double tagging is that an additional mass constraint (the second meson) is added. Searches with one missing particle per event (for example, a neutrino) only then become possible.

Achieving the high levels of background suppression by tagging while still retaining sensitivity to rare processes, implies the need for high tagging efficiencies through an optimized detector design.

Table III. Well-established single tag modes.

$D^0 \rightarrow$	BR	$\bar{\epsilon}$	# DET/yr
$K^- \pi^+$	0.042	0.61	2.7×10^6
$\bar{K}^0 \pi^0$	0.020	0.10	2.1×10^5
$\bar{K}^0 \pi^+ \pi^-$	0.064	0.14	9.4×10^5
$K^- \pi^+ \pi^0$	0.130	0.22	3.0×10^6
$K^- \pi^+ \pi^+ \pi^-$	0.091	0.35	3.3×10^6
$\bar{K}^0 \phi$	0.010	0.03	3.1×10^4
$\pi^+ \pi^-$	0.002	0.76	1.6×10^5
$K^+ K^-$	0.005	0.48	2.5×10^5
$K^- \pi^+ \pi^0 \pi^0$	0.149	0.08	1.2×10^6
Total			1.2×10^7
$D^+ \rightarrow$			
$\bar{K}^0 \pi^+$	0.0320	0.17	4.1×10^5
$K^- \pi^+ \pi^+$	0.091	0.53	3.6×10^6
$\bar{K}^0 \pi^+ \pi^0$	0.130	0.06	5.9×10^5
$\bar{K}^0 \pi^+ \pi^- \pi^+$	0.066	0.07	3.5×10^5
$K^+ K^- \pi^+$	0.011	0.42	3.5×10^5
$\bar{K}^0 K^+$	0.010	0.14	1.1×10^5
$K^- \pi^+ \pi^+ \pi^- \pi^+$	0.007	0.08	4.2×10^4
Total			5.5×10^6
$D_s \rightarrow$			
$\phi \pi^+$	0.030	0.14	1.1×10^5
$S^* \pi^+$	0.009	0.44	1.0×10^5
$\bar{K}^0 K^+$	0.030	0.22	1.7×10^5
$\eta \pi^+$	0.080	0.12	3.4×10^5
$\bar{K}^{0*} K^+$	0.030	0.14	1.1×10^5
Total			8.3×10^5

Table III summarizes the expectation for single tagging capabilities per year, in a detector only modestly improved in solid angle and particle identification over the Mark III.

The overall efficiency for tagging D^0 is conservatively estimated to be $\sim 12\%$, for $D^+ \sim 7\%$ and for $D_s \sim 3\%$. With improved photon detection efficiency, an additional factor of two in tagging efficiency may be possible.

The Pure Leptonic Decays

The pure leptonic decays of heavy mesons is at present a largely unexplored field. The diagrams for these decays are shown in Fig. 1. The partial width for these processes is proportional to the product of the weak hadronic current ($J_{hadronic}$) and the leptonic current ($J_{leptonic}$). The axial vector current $J_{hadronic}$ is defined by the Van Royen–Weisskopf equation:

$$\langle 0 | J_{hadronic}^\alpha | D^+ \rangle = iV_{cd}P^\alpha f_D \quad ,$$

in terms of the weak decay constant f_D of the D meson. The weak decay constant f_D is thus a fundamental constant which characterizes the degree of overlap of the heavy and light quarks in the meson. It contains all the QCD corrections which modify the $Wq\bar{q}$ vertex from a pure weak interaction. The weak decay constant can also be written in terms of wavefunctions of the heavy and light quarks, as:

$$f_D^2 = \frac{|\Psi(0)|^2}{M_D} \quad ,$$

emphasizing the overlap interpretation.

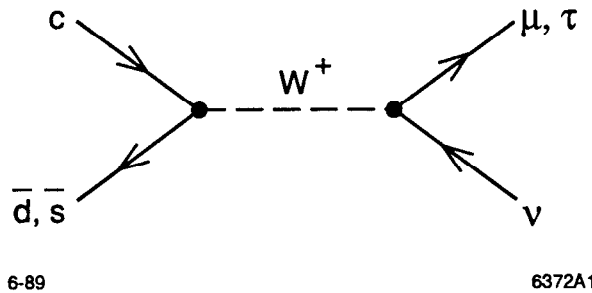


Figure 1: Diagram of the pure leptonic decays of the D^+ and D_s .

A measurement of the leptonic decay of the D^+ or D_s provides an unambiguous determination of f_D or f_{D_s} .⁷⁾

$$B(D^+ \rightarrow \mu^+ \nu) = \frac{\Gamma(D^+ \rightarrow \mu^+ \nu)}{\Gamma(D^+ \rightarrow \text{all})} = \frac{G_F^2}{8\pi} f_D^2 \tau_D M_D m_\mu^2 |V_{cd}|^2 \left(1 - \frac{m_\mu^2}{M_D^2}\right)^2,$$

where M_D is the meson mass; m_μ , the muon mass; V_{cd} , the Kobayashi–Maskawa (KM) matrix element; G_F , the Fermi constant; and τ_D , the lifetime of the D^+ .

In simple nonrelativistic quark models, decay constants should scale like the square root of the inverse of the heavy quark mass (the $1/M_D$ term) times the reduced mass of the heavy and light quark to a power between one and two [$\Psi(0)$ term]. This $1/M_D$ dependence appears to be reproduced in lattice calculations.⁸⁾ Thus, by measuring two distinct decay constants to adequate precision, say f_D and f_{D_s} , it should be possible to distinguish among models predicting their values, and then to reliably extrapolate to the even heavier B system for which experimental measurements may never be obtainable. Table IV summarizes some of the theoretical calculations of the decay constants.⁹⁾

Table IV. Theoretical estimates of weak decay constants.

Author	Year	Type	f_D	f_{D_s}	f_{B_d}	f_B/f_D
Mathur and Yamawaki	(81)	QCD SUM RULE	192	232	241	1.3
Aliev and Eletsii	(83)	QCD SUM RULE	170	–	132	0.8
Shifman	(87)	QCD SUM RULE	170	–	110/130	0.7/0.8
Narison	(87)	QCD SUM RULE	173	–	187	1.1
Dominguez and Paver	(87)	QCD SUM RULE	220	270	140/210	0.6/1.0
Reinders	(88)	QCD SUM RULE	170	–	132	0.8
Kraseman	(80)	POTENTIAL	150	210	125	0.8
Suzuki	(85)	POTENTIAL	138	–	89	0.6
Godfrey and Isgur	(85–86)	POTENTIAL	234	391	191	0.8
Bernard	(88)	LATTICE	174	234	105	0.6
DeGrand and Loft	(88)	LATTICE	134	157	–	–
Golowich	(80)	BAG	147	166	–	–

The importance of the weak decay constant goes beyond the pure leptonic decay process under discussion. Indeed, all the second-order weak processes involving hadrons—such as

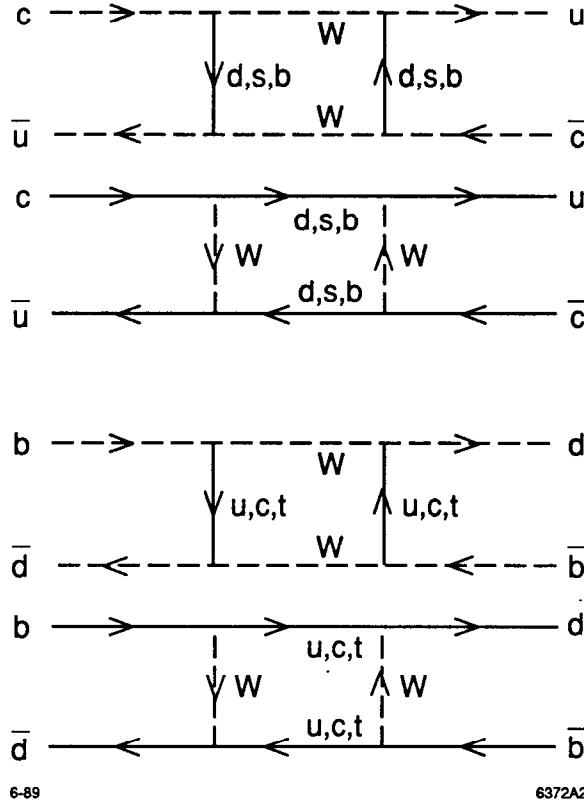


Figure 2: Box diagrams leading to $D^0\bar{D}^0$ and $B^0\bar{B}^0$ mixing.

$D\bar{D}$ and $B\bar{B}$ mixing involve box diagrams (see Fig. 2) whose evaluation requires the same understanding of QCD corrections to $J_{hadronic}$. In the case of the box diagrams, the mass eigenstate splitting which induces mixing in the B system is given by:

$$\frac{\Delta M_{B_d}}{\Gamma} \propto \tau_{B_d} M_t^2 M_{B_d} V_{tb} V_{td} (f_{B_d}^2 B_B) \eta_{B_d} F(M_t/M_W) .$$

The largest unknowns in this expression are the KM parameters, the B_d lifetime (τ_{B_d}), the decay constant f_{B_d} and the B_B parameter. The calculation of the B_B parameter is directly related to the calculation of the f_B , since it amounts to the QCD corrections (for internal gluon lines) to the box diagram. It is simply the ratio of the naive vacuum insertion calculation to the QCD corrected matrix element.

In a Tau-Charm Factory, the measurement of $D^+ \rightarrow \mu^+ \nu$, and $D_s \rightarrow \mu^+ \nu$ are straightforward.¹⁰⁾ Tagged events are sought, containing only one additional muon, and with missing mass near zero. The muon is monochromatic in the D rest frame, which is calculable from

the tag. After kinematic cuts from tagging, the major backgrounds that remain are from two-body hadronic channels and from real semimuonic decays. Both can be reduced to less than a few percent contamination by implementing a K_L^0 veto, and having good hermetic photon coverage. The pure leptonic decays $D_s \rightarrow \tau\nu$, with $\tau \rightarrow l\nu\nu$ or $\tau \rightarrow \pi\nu$ are also detectable, although the monochromatic nature of the lepton is lost; the missing mass constraint also is lost. There we rely on the tagging, hermeticity of the detector for photons, and the K_L^0 rejection. In addition, a large fraction of hadronic D_s decays with neutrals must be *independently measured* before interpretation of the result.

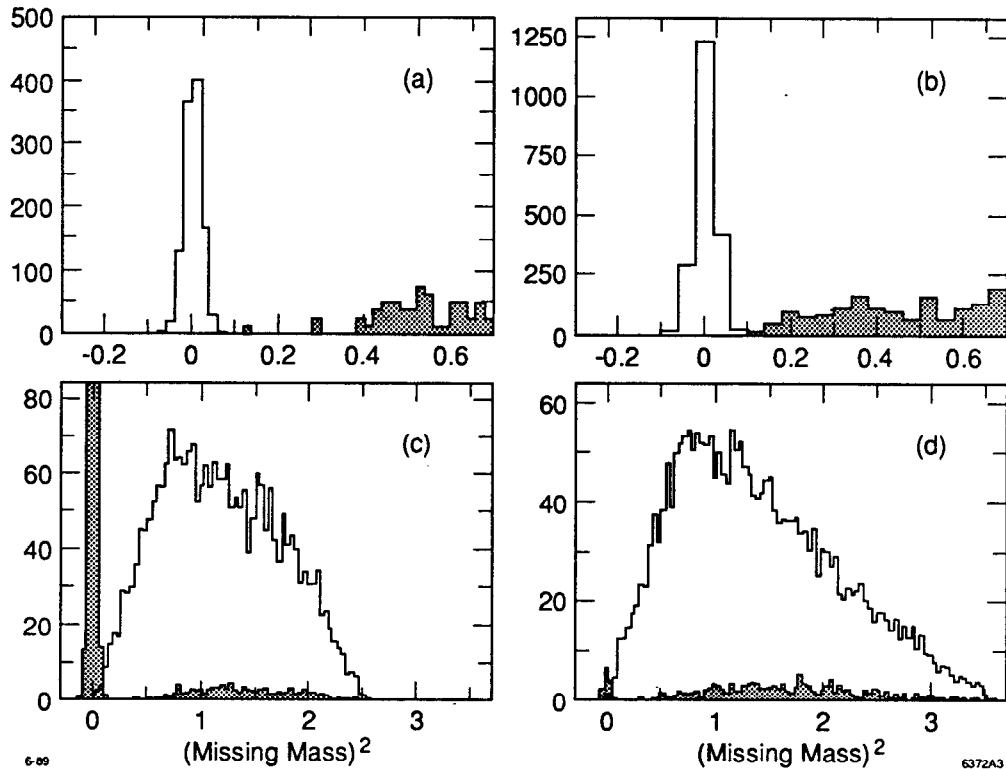


Figure 3: (a) Missing mass for $D^+ \rightarrow \mu\nu$, shaded areas are backgrounds; (b) missing mass for $D_s \rightarrow \mu\nu$; (c) missing mass for $D_s \rightarrow \tau\nu, \tau \rightarrow e\nu\nu$; and (d) missing mass for $D_s \rightarrow \tau\nu, \tau \rightarrow \mu\nu\nu$.

Figure 3 shows the four channels, with their backgrounds shaded, assuming a one-year run. Figure 4 shows an estimate for the number of reconstructed events in the three charmed meson channels. We would expect to measure f_D and f_{D_s} statistically to a few percent, and if all one-prong τ decays are usable, then $D_s \rightarrow \tau\nu$ is measurable and f_{D_s} can be reduced to a statistical error of about 1%. The systematic limitations of the measurement come from the

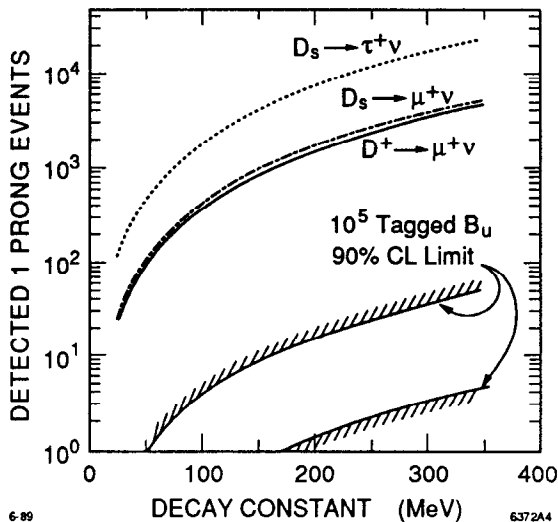


Figure 4: Detected pure leptonic events. Dotted ($D_s \rightarrow \tau\nu$); dot-dashed ($D_s \rightarrow \mu\nu$); solid ($D^+ \rightarrow \mu\nu$); limit region for $B \rightarrow \tau\nu$ based on 90% CL values of V_{bu} , assuming 10^5 tagged B_u and assuming the same detection efficiency as for the dotted line.

D meson lifetimes and knowledge of the KM matrix elements. Because this is theoretically the easiest calculation, as estimates improve, it may make sense to invert the procedure, using lattice theory for the ratio of f_D/f_{D_s} to extract the ratio of KM parameters V_{cd}/V_{cs} . Figure 4 also shows the expectation for a B factory where 10^5 B_u mesons have been tagged, and are used to measure $B \rightarrow \tau\nu$, assuming the same efficiency as the Tau-Charm Factory detector. Because of the small value of V_{bu} , this measurement does not appear feasible; however, if V_{bu} were large, and the $\tau\nu$ measurement could be made, a measurement of the lifetime of the B_u is also required to evaluate f_{B_u} .

In Fig. 1, only a W^+ was assumed to be exchanged. The diagram could equally well represent any charged scalar such as a nonminimal charged Higgs. Since a charged Higgs couples to a μ and τ with strengths proportional to their masses, the independent measurements of $D_s \rightarrow \tau\nu$ and $D_s \rightarrow \mu\nu$ can be compared, providing a very sensitive test of lepton universality and the presence of new currents. Higher-energy machines have been able to model dependently set limits down to 3 to 4 GeV, for a new scalar. These measurements are, however, at the edge of their detector resolution.¹¹⁾

Semileptonic Decays and Determination of the KM Matrix Parameters

At the present time, knowledge of the KM matrix in the first two generations is restricted to precision measurements in the kaon row alone. The values of V_{ud} and V_{us} are measured at the 0.1% and 1% level, respectively. Measurements in the charm row are only at the $\sim 20\%$ level now, dominated by statistics in some cases and systematics in others:

$$|V_{cd}|^2 = 0.058 \pm 0.014 \quad (\text{CDHS})$$

$$|V_{cs}|^2 = 0.530 \pm 0.080 \pm 0.060/f_+(0)^2 \quad (\text{MKIII})$$

$$|V_{cs}|^2 = 0.590 \pm 0.070 \pm 0.090/f_+(0)^2 \quad (\text{E691})$$

$$\left| \frac{V_{cd}}{V_{cs}} \right|^2 = 0.057_{-0.015}^{+0.038} \pm 0.005 \quad (\text{MKIII})$$

Beyond pure leptonic decays, the semileptonic Dl_3 decays provide the next level of difficulty for any theoretical interpretation. The partial width for Dl_3 decays involves two form factors $f_+(q^2)$ and $f_-(q^2)$, corresponding to the exchange of a vector meson. The latter is multiplied by the lepton mass squared in the matrix element and is normally dropped, leaving in the Cabibbo-allowed decays:

$$\Gamma(D \rightarrow Kl\nu) = \frac{G_F^2}{16\pi^3} M_D^5 |V_{cs}|^2 \int |f_+(q^2)|^2 (2x_e - 2x_K x_e - x_e^2 - 1 - \lambda^2) \quad .$$

In the simplest picture, $f_+(q^2)$ is represented as a simple pole, with one normalization constant $f_+(0)$:

$$f_+(q^2) = f_+(0) \left\{ \frac{M_{pole}^2}{M_{pole}^2 - q^2} \right\} \quad .$$

By systematically measuring the Dl_3 decay rates and the q^2 dependence of the form factors in D and D_s , it is possible to extract $V_{cd} \times f_+(0)$ and $V_{cs} \times f_+(0)$. Because $SU(4)$ is a badly broken symmetry, $f_+(0)$ deviates strongly from unity (unlike in the kaon system). Reliance on theory is imperative to extract the KM parameters. Ratios of rates will yield ratios of KM parameters with the form factor uncertainty reduced to the $SU(3)$ breaking level only ($\approx 5\%$). The theoretical values for $f_+(0)$ come from potential models, QCD sum rules, and lattice calculations (see Table V).¹²⁾

Table V. Recent theoretical estimates of $f_+(0)$.

Author	Year	Type	$f_+(0)$
Grinstein and Wise	(87)	NON. REL. POT.	0.58
Bauer, Stech and Wirbel	(85)	REL. POT.	0.73–0.75
Dominguez and Paver	(88)	QCD SUM RULE	0.75 ± 0.05
Soni and Bernard	(89)	LATTICE	0.75 ± 0.20

Figure 5 shows how semileptonic Cabibbo-allowed and Cabibbo-suppressed decays can be easily isolated using tagged events and plotting the missing energy less the missing momentum (the variable U). This is proportional to the missing mass in the event, peaking at zero for a single missing ν .

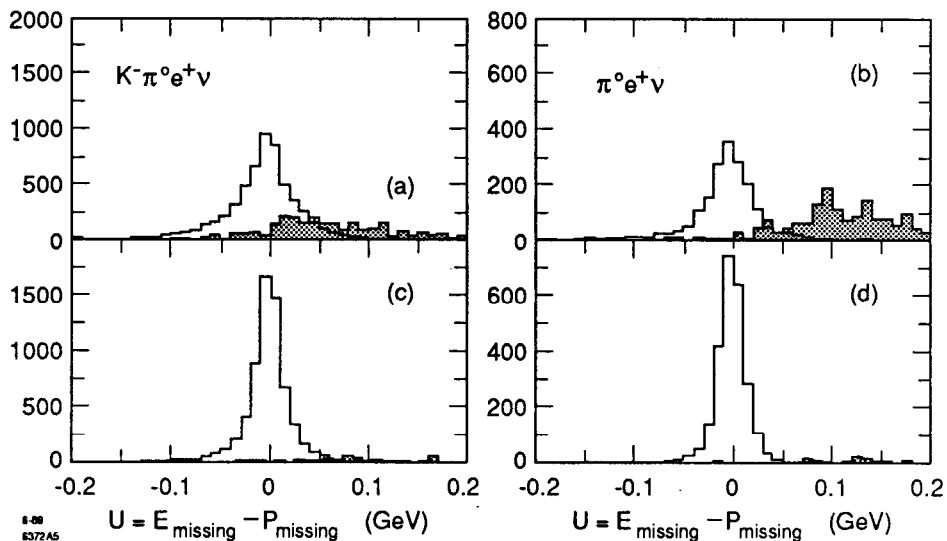


Figure 5: Cabibbo-allowed and Cabibbo-suppressed semileptonic decays.

In the Dl_4 decays, there are four form factors that appear; another vector $[V(q^2)]$ and three axial vector $[A_0(q^2), A_1(q^2), \text{and } A_2(q^2)]$. Again, one of these $A_2(q^2)$ is generally inaccessible, being multiplied by the square of a lepton mass. The overall q^2 dependence may be factored into a sum of simple pole-like terms and the matrix element formed in terms of two angles in the decay (θ, ϕ). These are the K or π decay angle (θ) in the K^* or ρ rest frame, and the angle (ϕ) of the decay plane of the W^+ ($\rightarrow l\nu$) relative to the decay plane of the K^* or ρ . Figure 6 shows the angles in the decay. Providing adequate statistics ($\sim 10^5$) are obtained,

measuring the Dl_4 decay rates and the q^2 dependence of the form factors in the (θ, ϕ) plane, allows one to determine the relative form factors and hence V_{cd} or V_{cs} up to a single constant.

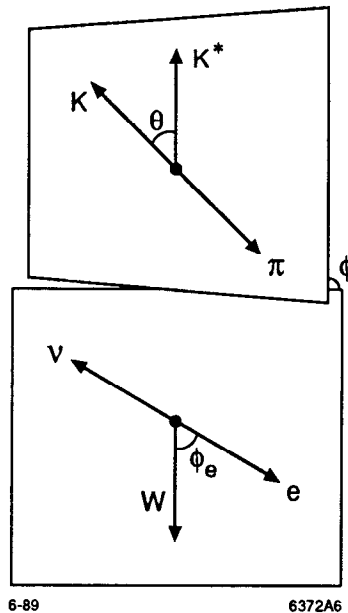


Figure 6: Decay plane decomposition in Dl_4 decays.

In Table VI, we estimate the expected rates for the numerous channels in the spectator-type semileptonic decays that are accessible to a Tau-Charm Factory.¹³⁾

The prescription for measuring V_{cd} and V_{cs} is thus to first measure the Dl_3 decays, comparing models for the form factors and adjusting models until shape agreement is reached. The same model is then tested against the Dl_4 decays, and similarly corrected until agreement is reached. In each case, both the allowed and Cabibbo-forbidden decays need to be examined. When a consistent model emerges, one can then reliably assume that the values of $f_+(0)$ can be used. Experimental statistical errors will be below 1%; then the partial width will be dominated from knowledge of the D and D_s lifetimes. On the timescale of the Tau-Charm Factory, $\sim 1\%$ absolute measurements of lifetimes may become available. If we only wish to constrain the ratios of KM angles, lifetime dependency is largely eliminated experimentally; it should be possible with many redundant measurements to reduce any residual detector systematics to the same level of $\sim 1\%$.

Table VI. Estimate for detection of exclusive semileptonic decays.

$D^0 \rightarrow$	BR	$\bar{\epsilon}$	# DET/yr
$K^- e^+ \nu$	0.034	0.71	0.29×10^6
$K^- \mu^+ \nu$	0.034	0.55	0.22×10^6
$K^{*-} e^+ \nu$	0.06	0.20	1.53×10^5
$K^{*-} \mu^+ \nu$	0.06	0.16	1.19×10^5
$\pi^- e^+ \nu$	0.004	0.80	0.37×10^5
$\pi^- \mu^+ \nu$	0.004	0.65	0.30×10^5
$\rho^- e^+ \nu$	0.004	0.33	0.16×10^5
$\rho^- \mu^+ \nu$	0.004	0.27	0.13×10^5
$D^+ \rightarrow$			
$\bar{K}^0 e^+ \nu$	0.07	0.82	0.11×10^6
$\bar{K}^0 \mu^+ \nu$	0.07	0.64	0.86×10^5
$K^{*0} e^+ \nu$	0.05	0.42	1.99×10^5
$K^{*0} \mu^+ \nu$	0.05	0.31	0.15×10^6
$\pi^0 e^+ \nu$	0.004	0.64	0.14×10^5
$\pi^0 \mu^+ \nu$	0.004	0.51	0.11×10^5
$\eta e^+ \nu$	0.0015	0.40	0.33×10^4
$\eta \mu^+ \nu$	0.0015	0.30	0.26×10^4
$\eta' e^+ \nu$	0.0005	0.30	0.92×10^3
$\eta' \mu^+ \nu$	0.0005	0.21	0.62×10^3
$\rho^0 e^+ \nu$	0.0025	0.95	0.13×10^5
$\rho^0 \mu^+ \nu$	0.0025	0.73	0.10×10^5
$\omega e^+ \nu$	0.0025	0.40	0.55×10^4
$\omega \mu^+ \nu$	0.0025	0.30	0.40×10^4
$F \rightarrow$			
$\eta e^+ \nu$	0.02	0.40	0.67×10^4
$\eta \mu^+ \nu$	0.02	0.30	0.51×10^4
$\eta' e^+ \nu$	0.006	0.40	0.15×10^4
$\eta' \mu^+ \nu$	0.006	0.21	0.85×10^3
$\phi e^+ \nu$	0.034	0.15	0.44×10^4
$\phi \mu^+ \nu$	0.034	0.11	0.32×10^4
$K^0 e^+ \nu$	0.002	0.82	0.47×10^3
$K^0 \mu^+ \nu$	0.002	0.64	0.36×10^3
$K^{*0} e^+ \nu$	0.0013	0.42	0.45×10^3
$K^{*0} \mu^+ \nu$	0.0013	0.31	0.34×10^3

In the next generation of experiments, before Tau-Charm, the KM parameters of the charm sector may be driven down below the 10% level with improved statistics. It remains unclear whether a sufficiently systematic and background-free set of measurements will become

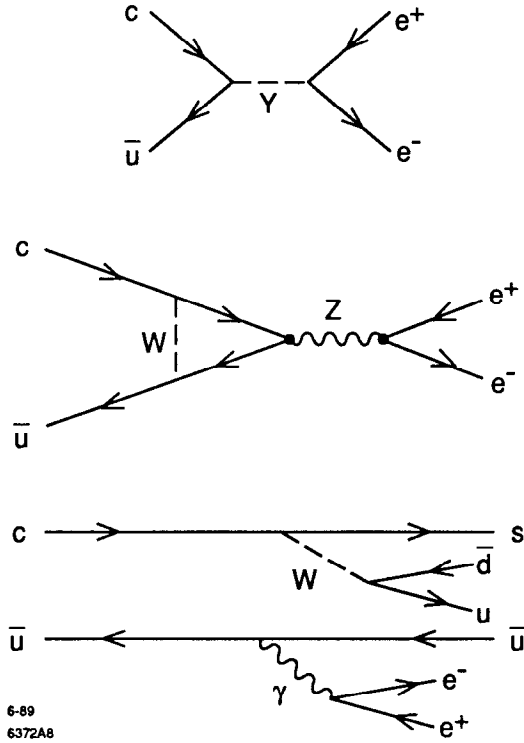


Figure 8: (a) Examples of flavor changing neutral currents involving new scalars or vectors; (b) and (c) are examples of allowed flavor-changing neutral currents.

rate signals the onset of New Physics. Examples are D^0 or $D^+ \rightarrow e^+ \mu^- X$, where X is a light hadron. Lepton family number-conserving decays (LFNC) can be simulated by effective flavor-changing neutral currents, allowed in the Standard Model *only* through higher order weak and/or electromagnetic processes [see, for example, Fig. 8(b)]. The simplest examples of such a processes are D^0 or $D^+ \rightarrow l^+ l^- X$. These one-loop induced FCNC are most susceptible to New Physics; they complement all searches in the down quark sector, because the couplings to new particles may be *a priori* flavor dependent, either through mass-dependent couplings or through mixing angles.

All of these classes of decays would be expected to occur at rates $\leq 10^{-7}$ in the Standard Model.¹⁵⁾ This generally occurs because of the need for a quark annihilation ($\sim f_D^2/M_D^2$) in the meson, and in the case of two-body decays, a further reduction occurring from the helicity suppression ($\sim M_l^2/M_D^2$) associated with the chirality of the leptons. Current estimates are that long-range effects may bring the Standard Model allowed processes up in rate to $(10^{-6}$

to 10^{-7}). If that is so, then correctly sorting New Physics from Old Physics will require the measurement of the full pattern of rare decays, each at the same sensitivity, rather than just limits or the observation of single isolated channels.

When helicity suppression is factored out of recent measurements—which are almost all limits at the few $\times 10^{-4}$ level¹⁶⁾—the mass reach of current measurements is about 0.2 TeV (choosing unit couplings for g_{qY} and g_{Yl}). As a result of the $1/M_Y^4$ dependence, sensitivity to a few TeV masses requires four orders-of-magnitude improvement over today's branching ratio measurements.

The Tau–Charm factory would gain an order of magnitude in sensitivity to M_Y , bringing us into the several TeV range for the helicity-suppressed class of rare decays. Luminosity alone provides about three orders of magnitude, and an improved detector which provides equal efficiency and background rejection to nonhelicity suppressed channels, will provide the balance. The nonhelicity suppressed channels provide sensitivity at the ~ 20 to 200 TeV scale, if unit couplings (g_{Yl} and g_{qY}) are assumed. Table VII shows the estimates for *signal sensitivity* to a set of rare decays.¹⁷⁾

Table VII. Rare decay sensitivity—preliminary analysis.

Channel	Estimated Background	Limit at 90% CL	Signal at 5σ
$D^0 \rightarrow e^+e^-$	≤ 0.2 events	3×10^{-8}	6.0×10^{-8}
$D^0 \rightarrow \mu^+e^-$	≤ 1.3 events	5×10^{-8}	1.2×10^{-7}
$D^0 \rightarrow \mu^+\mu^-$	≤ 10 events	8×10^{-8}	2.9×10^{-7}
$D^0 \rightarrow \rho^0 e^+e^-$	≤ 1.6 events	4×10^{-8}	1.3×10^{-7}
$D^0 \rightarrow K^0 e^+e^-$	≤ 1.5 events	2×10^{-7}	7.3×10^{-7}
$D^0 \rightarrow \nu\bar{\nu}$	≤ 22 events	–	8.0×10^{-6}

In addition to rare decays in the class described above, there are also ordinary radiative decays and penguin-type hadronic and radiative decays. An example of such penguin decays is shown in Fig. 9(a). The hadronic decays lead to ordinary Cabibbo-suppressed final states, and thus present a problem in untangling them from much larger “ordinary” physics.¹⁸⁾ The

electromagnetic penguins are GIM-suppressed¹⁹⁾ to a level of $O(10^{-8})$:

$$A \sim \frac{(m_s^2 - m_d^2)}{M_W^2} .$$

Rescattering processes (long-range effects) may, however, enhance the electromagnetic graphs to a level of $O(10^{-5})$. An example of rescattering through an intermediate state is shown in Fig. 9(b). Furthermore, a number of recent calculations suggest that QCD radiative corrections may enhance the penguin graph even further.²⁰⁾ At a level of 10^{-5} , decays like $D^+ \rightarrow \gamma \rho^+$ should be easily detectable in the Tau-Charm Factory.²¹⁾ Such a decay can be sought even in tagged events at that level, to entirely reduce noncharm backgrounds. The importance of seeking penguins in charm decay where the tree graph is below the sensitivity of the experiment is to establish the strength of long-range rescattering and QCD radiative corrections. Both these "corrections" must exist for B decay as well and, in fact, may compete (or even dominate) the t -quark contribution to the radiative penguin amplitude. Thus, if the class of penguin decays is found in D decay to be large [$O(10^{-5})$], it may be difficult to unambiguously untangle the t -quark contribution to an observed electromagnetic penguin B decay. Interestingly, CLEO or ARGUS have an excellent chance of first observing these B decays in the next few years.

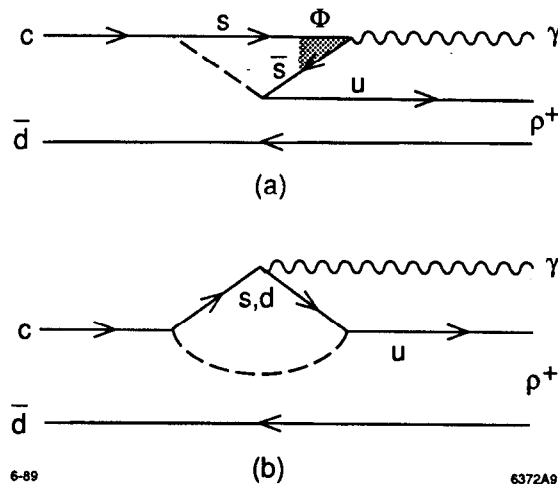


Figure 9: (a) Radiative penguin graph; (b) penguin final state simulated by a rescattering process.

Charm mesons may constitute the only system where Cabibbo-allowed, singly Cabibbo-suppressed, doubly Cabibbo-suppressed and second-order weak decays may be measured. While Tau-Charm can shed light on all of these measurements, space prevents the discussion here from going beyond the two rarest processes. In the Standard Model, $D^0\bar{D}^0$ mixing is a second-order weak interaction which occurs either through the twelve box diagrams [Fig. 10(a)] or through long-distance effects [Fig. 10(b)].²²⁾ The quantities ΔM and $\Delta\Gamma$ are the difference in mass and width between the weak-interaction eigenstates chosen to diagonalize the mass matrix describing the strong-interaction eigenstates (D^0 and \bar{D}^0) evolution. Experimentally, the mixing parameter r_D is defined as the number of observed events exhibiting mixing over the number of events not exhibiting mixing. In an experiment that does not measure time-evolution, but integrates over time, r_D is simply related to the mixing matrix parameters:

$$r_D = \frac{(\Delta M/\Gamma)^2 + (\Delta\Gamma/2\Gamma)^2}{2}$$

The box diagram contributions to mixing are expected to be small $r_D \leq 10^{-6}$ because of GIM cancellations. Long-range contributions (also second-order weak) to r_D from ΔM and $\Delta\Gamma$ may be equal in magnitude and each as large as $\sim \text{few} \times 10^{-2}$. These large contributions may come about from SU(3) breaking and differences in partial widths to intermediate CP eigenstates.²³⁾

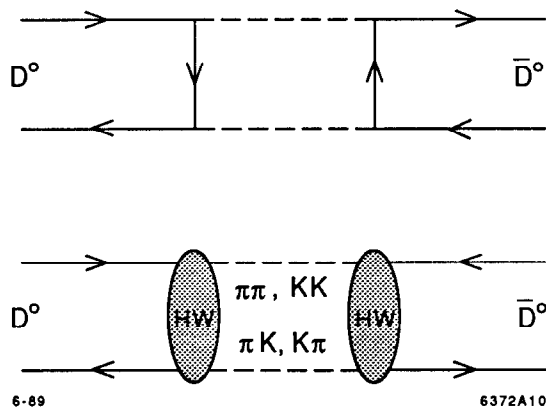


Figure 10: (a) $D^0\bar{D}^0$ mixing from box diagrams; and (b) from long-range effects.

At this large α_s level, one of the main experimental backgrounds leading to “mixing-like” final states comes from doubly Cabibbo-suppressed decays (DCSD). Having branching fractions of $O(\tan^4 \theta_c) = 0.003$, these decays may dominate a mixing signature. In the absence of time-evolution information, it has been suggested by Bigi¹⁹⁾ that a set of measurements at two or more energies can be used in conjunction with quantum statistics to sort out mixing from DCSD or New Physics. It is also possible, using the interference term, to measure $\Delta M/\Gamma$ and $\Delta\Gamma/\Gamma$ separately. This is illustrated in Table VIII, where two such sets of measurements are made. First, final states where both D^0 mesons decay semileptonically (thereby eliminating DCSD background), and second, where both decay hadronically, but to identical final states. In the latter case, Bose statistics forbids DCSD when the D^0 mesons are in a relative $l = 1$ state. When the D^0 are in a $l = 0$ state, then mixing and DCSD interfere, allowing a measurement of both. A third possible option to sort out mixing and DCSD is to measure a semileptonic decay versus a hadronic decay.

Table VIII. Establishing mixing contributions and DCSD.

$e^+e^- \rightarrow$	No Mixing Signature (No New Physics)	Mixing Signature
$D^0\bar{D}^0$	$\frac{K^\mp\pi^\pm K^\mp\pi^\pm}{K^-\pi^+ K^+\pi^-}$ 0	r_D
$D^0\bar{D}^0 \gamma$	$4 \tan^4 \theta_c \hat{\rho} ^2$	$3r_D + 8 \left(\frac{\Delta\Gamma}{2\Gamma}\right) \tan^2 \theta_c \hat{\rho} + 4 \tan^4 \theta_c \hat{\rho} ^2$
$D^0\bar{D}^0 \pi^0$	0	r_D
$D^0\bar{D}^0$	$\frac{K^\mp l^\pm K^\mp l^\pm}{K^\mp l^\pm K^\pm l^\mp}$ 0	r_D
$D^0\bar{D}^0 \gamma$	0	$3r_D$
$D^0\bar{D}^0 \pi^0$	0	r_D

In Table VIII, the quantity $\hat{\rho}$ is defined by Bigi’s convention:

$$\hat{\rho} = \frac{1}{\tan^2 \theta_c} \frac{\text{T}(D^0 \rightarrow K^+\pi^-)}{\text{T}(D^0 \rightarrow K^-\pi^+)} .$$

Note that the doubly Cabibbo-suppressed amplitudes can be measured in parallel with tagged events (see below).

At a Tau-Charm Factory, our preliminary analysis suggests that we can reconstruct at the $\psi(3770)$ in excess of 1.80×10^5 events in the two categories of Table VIII.²⁴⁾ Backgrounds appear to be reducible by a combination of detector particle identification and kinematic constraints. At any of the higher energies suggested (4.03 or 4.14 GeV/c²), providing photon detection efficiency and resolution are comparable to that achieved in current "crystal" calorimeters, similar numbers of events should be reconstructable, including the $D^{*0} \rightarrow \gamma D^0$ or $D^{*0} \rightarrow \pi^0 D^0$. At least one study has been done to verify this conclusion.²⁵⁾ Similar studies using $D^{*+} \rightarrow \pi^+ D^0$ have also been done. They conclude that if either the whole event is reconstructed (the D^+ tag and the recoil), or at most the soft π^+ is lost,²⁶⁾ this flavor-tagging scheme would appear to have statistical power similar to the experimental results shown in Table VIII. This implies that at a Tau-Charm Factory, $D^0 \bar{D}^0$ mixing should be *measurable* at the level of $r_D \approx 10^{-4}$, and unambiguously *observable* at the level of $r_D \approx 10^{-5}$, by several independent techniques.

A clear understanding of DCSD can be reached by measuring D^+ decays, where the signature is not confused by a mixing component present in D^0 decays. D^+ DCSD have an added attraction, because unlike allowed D^+ decays, they do not suffer from interference effects, and hence may be significantly enhanced. This was first noted by I. I. Y. Bigi.¹⁹⁾ At the present time, no experiment has yet reported clear evidence for D^0 or D^+ DCSD. One of the severe experimental problems is the kinematic reflection from nonsuppressed decays. Table IX gives estimates of some of the DCSD modes of the D^+ (see Ref. 21).

Preliminary studies²⁷⁾ suggest that the background in the largest channels can be reduced below 10% with a modest improvement in particle identification and momentum resolution.

Conclusions

The Tau-Charm Factory will combine a high-luminosity collider and dedicated injector to optimize average luminosity close to peak luminosity. Drawing on experience from all previous generations of detectors at SPEAR, it is clear that a new detector that marries highly efficient, fine-grained electromagnetic calorimetry (while retaining good angular resolution)

Table IX. Estimates of double cabibbo-suppressed D^+ decays:

$$L = 10^{33} \text{ cm}^{-2} \text{ sec}^{-1}.$$

Channel $D^+ \rightarrow$	$\bar{\epsilon}$ (est.)	$\tan^4 \theta_c$ coeff.	Events Detected
$K^+\pi^0$	0.43	0.02	142
$K^+\eta$	0.09	0.01	15
$K^+\eta'$	0.04	0.01	6
$K^+\omega$	0.34	0.01	56
$K^+\rho^0$	0.42	0.07	498
$K^{*0}\pi^+$	0.28	0.06	232
$K^{*0}\rho^+$	0.25	0.01	42
$K^{*+}\pi^0$	0.13	0.05	106
$K^{*+}\eta$	0.03	0.02	9
$K^{*+}\eta'$	0.01	0.02	4
$K^{*+}\omega$	0.11	0.01	18
$K^{*+}\rho^0$	0.13	0.01	22
$K^+\pi^-\pi^+$	0.42	0.07	512

to a precision low-mass tracker would provide a significant improvement in the efficiency for tagging charmed events over any earlier detector. Coupled with a redundant particle identification system and a unique hermetic hadron (K_L^0) veto system, the collider and the detector should be able to probe the region of the physics of charm decays lying about three orders-of-magnitude lower than our present measurements.

Acknowledgments

I would like to thank the organizers for putting together an extremely stimulating conference; both the physics and the culinary aspects of the meeting set a new standard for the field.

I would also like to thank certain members of my group (T. Browder, U. Karshon, P. Kim, and D. Pitman) as well as my collaborators, G. Gladding, J. Izen, A. Seiden, and C. Simopoulos, all of whom played an important role in providing much of the information referenced in this report. Finally, I would like to thank I. Bigi, B. Ward, and R. Willey for many valuable discussions.

REFERENCES

1. M. Perl, The Tau-Charm Factory Concept, these proceedings.
2. Several possible injector designs were evaluated at the Tau-Charm Workshop, all delivering e^+ and e^- for fills in less than 60 seconds. Beam lifetimes are estimated to be 140 minutes.
3. We assume eight months per year of high energy physics; 85% of that corresponds to 5000 hrs.; two months of machine physics and two months of scheduled downtime.
4. The one exception is $D_s\bar{D}_s$ at $4.028 \text{ GeV}/c^2$. There, we have used a theoretical estimate from coupled channel potential models, fit to D meson data in the vicinity to establish the cross section.
5. R. M. Baltrusaitis *et al.*, *Phys. Rev. Lett.* **54** (1985) 1976.
6. R. M. Baltrusaitis *et al.*, *Phys. Rev. Lett.* **55** (1985) 150.
7. E. D. Commins and P. H. Bucksbaum, *Weak Interactions of Leptons and Quarks*, (Cambridge University Press, Cambridge, UK, 1983) pp. 155–156.
8. A. Soni, private communication; and
C. Bernard *et al.*, *Phys. Rev.* **D38** (1988) 3540.
9. H. Krasemann, *Phys. Lett* **96B** (1980) 397;
E. Golowich, *Phys. Lett.* **91B** (1980) 271;
V. Mathur *et al.*, *Phys. Lett.* **107B** (1981) 127;
T. Aliev *et al.*, *Sov. J. Nucl. Phys.* **38** (1983) 6;
M. Suzuki, *Phys. Lett.* **142B** (1984) 207;
S. Godfrey *et al.*, *Phys. Rev.* **D32** (1985) 189;
S. Godfrey, *Phys. Rev.* **D33** (1986) 1391;
C. Dominguez *et al.*, *Phys. Lett.* **197B** (1987) 423;
L. Reinders, *Phys. Rev.* **D38** (1988) 947;
C. Bernard *et al.*, *Phys. Rev.* **D38** (1988) 3540;
T. DeGrand *et al.*, *Phys. Rev.* **D38** (1988) 954.

10. P. Kim, *Proceedings of the Tau-Charm Workshop*, SLAC-REPORT-343, Vol. 1 (1989).
11. W. Bartel *et al.*, *Z. Phys.* **C31** (1986) 359.
12. C. Bernard *et al.*, *Phys. Rev.* **D38** (1988) 3540;
 C. Dominguez *et al.*, *Phys. Lett.* **207B** (1988) 499;
 C. Dominguez *et al.*, *Phys. Lett.* **197B** (1987) 423;
 B. Grinstein *et al.*, *Phys. Rev.* **D39** (1989) 799;
 B. Grinstein *et al.*, *Phys. Rev. Lett.* **56** (1986) 298;
 B. Grinstein *et al.*, CALTECH 68-1311 (1986);
 M. Bauer *et al.*, *Z. Phys.* **C29** (1985) 637.
13. J. Izen, *Proceedings of the Tau-Charm Factory Workshop*, SLAC-REPORT-343, Vol. 1 (1989).
14. I. I. Y. Bigi, *Proceedings of the 16th SLAC Summer Institute* (1988) 30.
15. R. Willey, *Proceedings of the Tau-Charm Factory Workshop*, SLAC-REPORT-343, Vol. 1 (1989);
 I. I. Y. Bigi, *Proceedings of the 16th SLAC Summer Institute* (1988) 30.
16. C. Grab, *Proceedings of the Rare Decay Symposium*, Vancouver, Canada, November 30-December 3, 1988. Also, SLAC-PUB-4809.
17. I. Stockdale, *Proceedings of the Tau-Charm Workshop*, SLAC-REPORT-343, Vol. 1 (1989).
18. P. X. Yen, *Modern Phys. Lett.* No. 11 (1986);
 J. Finjord, *Nuclear Phys.* **B181** (1981) 74.
19. See the discussion in I. I. Y. Bigi, Ref. 14.
20. See, for example, B. Grinstein *et al.*, *Phys. Lett.* **202B** (1988) 138.
21. T. Browder, *Proceedings of the Tau-Charm Factory Workshop*, SLAC-REPORT-343, Vol. 1 (1989).
22. L. Wolfenstein *Phys. Lett.* **164B** (1985) 170;
 J. Donoghue *et al.*, *Phys. Rev.* **D33** (1986) 179.

23. For a detailed discussion, see H. Yamamoto, CALTECH 68-1318 (1986).
24. G. Gladding, *Proceedings of the Tau-Charm Workshop*, SLAC-REPORT-343, Vol. 1 (1989).
25. U. Karshon, *Proceedings of the Tau-Charm Workshop*, SLAC-REPORT-343, Vol. 1 (1989).
26. C. Simopoulos, *Proceedings of the Tau-Charm Workshop*, SLAC-REPORT-343, Vol. 1 (1989).
27. Our conclusion is based on studies originally done with the Mark III detector.